Strong interplay between electron-phonon interaction and disorder in low doped systems

Domenico Di Sante[1, 2] and Sergio Ciuchi[1, 3, 4]

[1]*University of L'Aquila, Department of Physical and Chemical Sciences, Via Vetoio, L'Aquila, Italy*
[2]*CNR-SPIN, Via Vetoio, L'Aquila, Italy**
[3]*CNISM Udr L'Aquila*
[4]*CNR-ISC, Via dei Taurini, Rome, Italy*†

The effects of doping on the spectral properties of low doped systems are investigated by means of Coherent Potential Approximation to describe the distributed disorder induced by the impurities and Phonon-Phonon Non-Crossing Approximation to characterize a wide class of electron-phonon interactions which dominate the low-energy spectral features. When disorder and electron-phonon interaction work on comparable energy scales, a strong interplay between them arises, the effect of disorder can no more be described as a mere broadening of the spectral features and the phonon signatures are still visible despite the presence of strong disorder. As a consequence, the disorder-induced metal-insulator transition, is strongly affected by a weak or moderate electron-phonon coupling which is found to stabilize the insulating phase.

PACS numbers: 63.20.kd,73.20.Hb,74.25.Jb

I. INTRODUCTION

In the last years the developement of more accurate methods of investigations such as Angular Resolved PhotoEmission Spectroscopy (ARPES), joined with the fabrication of novel materials as high-Tc superconductors[1,2], colossal magnetoresistance manganites[3], correlated oxides[4], topological insulators[5] and graphene[6] in different topological conditions (from bulk, to surfaces and eterostructures, up to single monolayers), allowed a deep insight in low-energy electronic and spectral properties. The countinuosly increased measurements' accuracy in experiments gives the opportunity to detect and study such low-energy features which in many cases were recognized as the fingerprint of the electron-phonon interaction.

The possibility to tune the chemical potential by doping offers a great potentially useful way to modify the materials' electronic structures and properties. Very recently, in the low doping conditions electron-phonon signatures were successfully detected in the ARPES spectra of many different systems, from oxygen vacancies doped $SrTiO_3$ surface[7] or lightly bulk doped $SrTiO_3$[8,9], to monolayer pnictide $FeSe$ growth on $SrTiO_3$[10], from tridimensional Anatase[11] to $Ba_{1-x}K_xBiO_3$[12] and $Cu_xBi_2Se_3$[13] superconductors, up to Z_2 topological non-trivial materials as Bi_2Se_3 and Bi_2Te_3[13], as well as on the quasi two-dimensional layered lightly-doped Sr_2TiO_4[14]. Such a rich variety of different materials displaying common electron-phonon low-energy features calls for a deeper understanding of the underlying mechanism at play. However, once all these systems are taken into account and in particular when dealing with surfaces, monolayers and low-dimensional systems, the role of disorder cannot be neglected. In fact the growth processes on substrates and/or the action of chemical doping imply the presence of disorder, whose impact largely depends on which energy scale one is focused on. For example, impurity bands can be formed close to the conduction band of the pristine material as a consequence of the presence of the dopant energy levels[14,15], or can have magnetic origins as in Mn-doped GaAs[16,17]. On the other hand, oxygen vacancies on the substrate[7] may represents centers of scatterings for carriers in the deposited film. Interestingly in this sense, recent ARPES experiments and ab-initio theoretical works suggest how charge carriers can be trapped by oxygen vacancies at the $LaAlO_3/SrTiO_3$ (LAO/STO) interface[18] and $SrTiO_3$ surface[19,20], naturally introducing the role of disorder in the understanding of the electronic properties of oxide-oxide heterostructure interfaces and oxide surfaces, where confined two-dimensional electron gases (2DEGs) should also undergo superconducting phase transitions[21].

Usually disorder can be added perturbatively in the theoretical explanation of ARPES spectra as a weak source of scattering leading to an intrinsic band linewidth. Within this approach, interactions such as electron-phonon coupling contribute to the low-energy properties of the spectrum and the disorder simply provides a further smearing of the electron-phonon features. However this is not the case when disorder and electron-phonon interaction act on comparable energy scales. For example let us consider the case of an intermediate electron-phonon coupling; in the very low doping limit, the system is prone to polaron formation and the presence of scattering centers may provide, in a synergic way, the necessary energy to stabilize a small polaron[22–26]. Another example is that of a low (but finite) electron density and weak electron-phonon coupling. In this case when disorder and electron-phonon interaction are treated self-consistently impurity and phonon contributions to electron scattering are not additive when the Fermi energy is of the order of the phonon frequency[27,28], and impurity scattering has a significant nonlinear effect[29]. In this work we approach the problem of the interplay between disorder and electron-phonon interaction starting from a weak electron-phonon coupling, going beyond the self-consistent Born approximation used in refs.[27–29] by using the Coherent Potential Approximation (CPA) thus extending our treatement to the case of strong disorder. Previous studies of models in this peculiar regime concentrated on the case of classical phonons in binary alloys[30] or, in the same context, on the effects of electron-phonon interaction on transport properties at high temperature[31]. Electron-phonon interaction and strong disorder have also been studied in the classical phonon case[32] within the context of the Falicov-Kimball model of correlated electrons, for which CPA is the exact solution[33]. Noticeably, the Mott transition in the Falicov-Kimball model can be described as a disorder-induced metal-insulator transition (MIT) in the alloy context[33]. Here we address the single particle properties, namely how disorder and electron-phonon interaction modifies ARPES spectra of lightly-doped materials[34]. A proper quantum treatment of the phonon is, in this case, crucial to explain the low energy features of ARPES spectra. The disorder-induced metal-insulator transition is also studied as it depends on the strength of the electron-phonon interaction.

The paper is organized as follows: in Section II we discuss the model Hamiltonians and the types of electron-phonon couplings taken into account in this work. In Section III we explain how such models can be solved in presence of local disorder as introduced by an Anderson type Hamiltonian, and we discuss the fluctuation of the electron-phonon self-energy due to disorder. In Section IV we present the main results of our work discussing the interplay between electron-phonon interaction and disorder to explain the features of the ARPES spectra, we discuss also the electron-phonon dependence of the disorder-induced metal-insulator transitiion. In Section V we draw our conclusions and further remarks.

II. MODEL HAMILTONIANS

We consider in this work an Anderson type Hamiltonian for twodimensional tight-binding electrons interacting with dispersionless optical phonon modes of the general form

$$H = H_{el} + H_{ph} + H_{e-ph} + H_{dis} \quad . \tag{1}$$

The electronic nearest-neighbor tight-binding part $H_{el} = -t \sum_{<i,j>} (c_i^\dagger c_j + h.c.)$ gives rise to a twodimensional energy dispersion $\varepsilon_k = -2t(\cos k_x + \cos k_y)$; $c_i^\dagger$ and c_i are the charge carrier creation and annihilation operators, respectively. The half-bandwidth $D = 4t$ will be the energy unit throughout the paper and all k-vectors are given in units of π/a where a is the lattice spacing. We also choose the zero energy level $\omega = 0$ to the position of the chemical potential.

The disorder part is assumed to be of the Anderson type

$$H_{dis} = \sum_i \xi_i c_i^\dagger c_i \quad , \tag{2}$$

where ξ_i are disorder independent random energies taken according to the following disorder distributions:
i) the bimodal $P_i(\xi) = x\delta(\xi - E_b) + (1-x)\delta(\xi)$ characterizing a concentration of x impurities in the host material,
ii) the gaussian $P_g(\xi) = (1/\sqrt{2\sigma^2})\exp(-\xi^2/2\sigma^2)$ where σ^2 is the disorder variance to mimic a conformational disorder,
iii) or as the sum of two independent variables, one of which distributed according to P_i, and the other one distributed according to P_g.

For the free phonon part, we assume a simple undispersed Einsteins' phonon Hamiltonian $H_{ph} = \omega_0 \sum_i a_i^\dagger a_i$ with a characteristic phonon frequency ω_0. We fix the value of the phonon frequency in the adiabatic regime $\omega_0/D = 0.05$.

For the electron-phonon interaction part H_{e-ph} we consider three different kinds of models. The first two can be obtained from the following density-displacement Hamiltonian

$$H_{e-ph} = -\sum_{i,j} g_{i,j} c_i^\dagger c_i (a_j + a_j^\dagger) \quad . \tag{3}$$

The Holstein local (LOC) model is obtained when $g_{i,j} = g\delta_{i,j}$, whereas a general, even long-range Fröhlich type interaction (NLOC), can be considered in more general cases. In the spirit of our work, here we focus our attention on the two-dimensional screened Fröhlich type interaction. Let us consider the long wavelength limit of the Fourier transform of the longitudinal optic (LO) polar coupling $[g^2]_{i,j} = \sum_k g_{i,k} g_{k,j}$

$$g^2(\mathbf{k}) = \frac{1}{N} \sum_R e^{-i\mathbf{k}\mathbf{R}} [g^2]_{i,i+R} \quad . \tag{4}$$

If $g^2(\mathbf{k})$ is of the Fröhlich type, i.e. $g^2(\mathbf{k}) \propto 1/k^2$, after summing over all possible value of k_z, we get an effective coupling which at small k behaves as $g^2(\mathbf{k}) \propto 1/k$ depending only on the two-dimensional wave-vector $\mathbf{k}$ [35]. Since in our model electrons are free to have planar motions, we next consider the action of the two-dimensional screening of the in-plane carriers. This screening is independent on the carrier density, and the effective coupling is thus replaced by $g^2(\mathbf{k}) \to g^2(\mathbf{k})/\epsilon(\mathbf{k}, \omega = 0)$, where $\epsilon(\mathbf{k}, \omega = 0) = 1 + \kappa/k$ and $\kappa = 2m^* e^2/\hbar^2 \epsilon_r$ is the two-dimensional screening wave-vector. The large k behaviour of $g^2(\mathbf{k})$ is obtained restoring the lattice symmetries by replicating the small k form

$$g^2(\mathbf{k}) = \frac{C}{N_\mathbf{G}} \sum_\mathbf{G} \frac{|\mathbf{k} + \mathbf{G}|}{|\mathbf{k} + \mathbf{G}| + \kappa} \tag{5}$$

where $\mathbf{G}$ is a reciprocal lattice vector and $N_{\mathbf{G}}$ is the number of summed terms in eq. (5). For our aims, we find that a summation over the nearest-neighbor reciprocal vectors is sufficient. The normalization constant C is chosen by fixing the value of a coupling constant g

$$g^2 = \frac{1}{N}\sum_{\mathbf{k}} g^2(\mathbf{k}) \quad . \tag{6}$$

In both LOC and NLOC models the dimensionless electron-phonon coupling constant is defined in terms of g as

$$\lambda = 2g^2/\omega_0 D \quad . \tag{7}$$

Another model which we consider in this work is the so-called interaction with a phonon mode such as that occurring with apical oxygens in layered perovskites[36], to which hereafter we refer as Apical Oxygens Hamiltonian (AO)[37]. The form of the Hamiltonian is the same as in eq. (1), but now we consider several two-dimensional planes where electron carriers are free to move (index α) unconnected by out-of-plane hopping processes. The interaction between different planes is introduced through the following AO electron-phonon coupling

$$H^{BM}_{e-ph} = -\frac{g}{\sqrt{2}}\sum_{i.\alpha} c^\dagger_{i,\alpha}c_{i,\alpha}(x_{i,\alpha+1/2} - x_{i,\alpha-1/2}) \quad , \tag{8}$$

where $x_{i,\alpha+1/2}$ is the (dimensionless) displacement $x_{i,\alpha+1/2} = (a^\dagger_{i,\alpha+1/2} + a_{i,\alpha+1/2})$ of the interplane apical atom in the i-th site of the α-th plane. Within this AO model, disorder variables are chosen uncorrelated as before, and the Anderson term now reads as $H^{BM}_{dis} = \sum_{i,\alpha}\xi_{i,\alpha}c^\dagger_{i,\alpha}c_{i,\alpha}$. In AO model the dimensionless electron-phonon coupling constant is defined as in the LOC and NLOC models through Eq. (7).

III. METHODS OF SOLUTION FOR LOCAL AND NON-LOCAL ELECTRON-PHONON HAMILTONIANS

A. CPA and Phonon-Phonon Non-Crossing Approximation in the Holstein model

Here we introduce our approximations in the case of purely local electron-phonon interaction (LOC). We use the CPA to treat the local disorder. The CPA can be thought as an exact theory on an infinite coordination lattice[38]; for this reason it is therefore much similar to the single-site Dynamical Mean Field Theory (DMFT)[39,40]. As in DMFT, for solving the LOC model we consider a single site embedded into a self-consistent medium[40]. The single-site propagator $\mathcal{G}$ can be expressed in terms of a local propagator which embodies the *average* action of the environment ($G_0(\omega)$) and a self-energy $\Sigma(\omega)$[40]:

$$\mathcal{G}(\omega) = \frac{1}{G_0^{-1}(\omega) - \Sigma(\omega)} \quad . \tag{9}$$

The site propagator $\mathcal{G}$ can be expressed as an average over disorder variable (hereafter a generic quantity A which depends on disorder realizations is denoted by $\hat{A}$ while its average is $A = [\hat{A}]_\xi$)

$$\mathcal{G}(\omega) = \left[\frac{1}{G_0^{-1}(\omega) - \xi - \hat{\Sigma}_{eph}(\omega)}\right]_\xi \quad , \tag{10}$$

where ξ is the local disorder variable and $\hat{\Sigma}^{eph}(\omega)$ is the electron-phonon self-energy which depends on the local disorder variables.

Electron-phonon interaction in the LOC model can be self-consistently taken into account within a CPA — or equivalently DMFT — scheme at zero electron density[41]. At finite electron density we choose a self-consistent Phonon-Phonon Non-Crossing Approximation (PPNCA) for the electron-phonon self-energy[42] (see diagrams of type a) in Fig. 1):

$$\begin{aligned}\hat{\Sigma}_{eph}(\omega) &= -\frac{g^2}{\beta}\sum_m D^0(\omega - \imath\omega_m)\hat{\mathcal{G}}(\imath\omega_m) \\ &+ \hat{\Sigma}_H \quad ,\end{aligned} \tag{11}$$

where $D^0(\omega)$ is the free-phonon Green's function while the frequency independent Hartree term of the electron-phonon self-energy

$$\hat{\Sigma}_H = -\frac{2g^2}{\omega_0}\hat{n} \tag{12}$$

is expressed in term of the local density $\hat{n}$ which is given by $\hat{n} = -\frac{1}{\beta}\sum_n \hat{\mathcal{G}}(\imath\omega_n)e^{i\omega_n 0^+}$. In this approximation the phonon propagator is not renormalized by the electron density fluctuations; we therefore associate the phonon frequency to that obtained by experiment or assume that the phonon frequency renormalization is negligible at low electron density.

After Matsubara's frequency summation the PPNCA self-energy is written as

$$\begin{aligned}\hat{\Sigma}_{eph}(\omega) = g^2\int d\epsilon\hat{A}(\epsilon)\left[\frac{b(\omega_0)+f(\epsilon)}{\omega+\omega_0-\epsilon+\imath\delta} + \right. \\ \left. \frac{b(\omega_0)+1-f(\epsilon)}{\omega-\omega_0-\epsilon+\imath\delta}\right] + \hat{\Sigma}_H \quad ,\end{aligned} \tag{13}$$

with $b(\omega_0)$ and $f(\epsilon)$ referring to the Bose-Einstein and Fermi-Dirac distributions respectively, and $\hat{A}(\epsilon) = (-1/\pi)\Im\hat{\mathcal{G}}(\epsilon)$ being the spectral function.

The averaged propagator is translationally invariant. It can be expressed in terms of the local self-energy as: $G(k,\omega) = 1/[\omega - \epsilon_k - \Sigma(\omega)]$. The averaged local propagator is thus:

$$G_{loc}(\omega) = \int d\epsilon N(\epsilon)\frac{1}{\omega - \epsilon - \Sigma(\omega)} \quad , \tag{14}$$

where $N(\epsilon) = \sum_k \delta(\epsilon - \epsilon_k)$ is the non-interacting density of states. The self-consistency condition requires the single-site Green's function (10) to coincide with the local lattice Green's function (14)

$$G_{loc}(\omega) = \mathcal{G}(\omega) \quad . \tag{15}$$

In this way equations (9,10,13,14,15) define a self-consistency loop to be iterated to get the self-consistent local self-energy which takes into account disorder at the CPA level as well electron-phonon interaction coming only from diagrams of type a) in Fig. 1. We call this scheme PPNCACPA. From the operative point of view, starting with an educate ansatz for G_0, we use Eqs. (10,13) to determine $\mathcal{G}$, Eq. (15) to obtain Σ and Eq. (9) to obtain a new G_0 for iterating the procedure. This iteration scheme differs from DMFT due to the approximate treatment of the electron-phonon interaction trough PPNCA.

B. PPNCACPA in the AO model

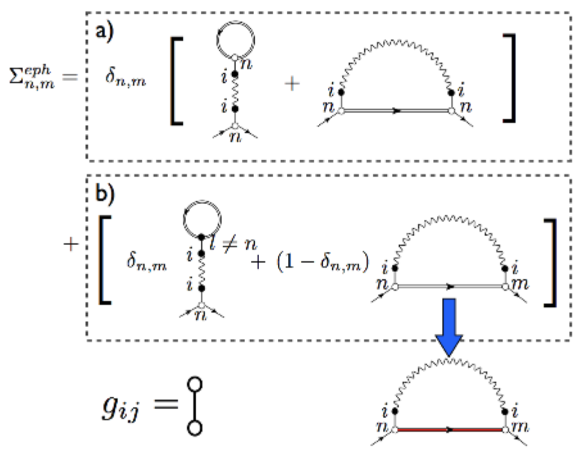

FIG. 1: Electron-phonon interaction diagrams. Open straight line is the non-averaged electron propagator, filled straight line is the disorder-averaged electron propagator, wavy line is the phonon porpagator.

To generalize PPNCACPA to the AO model we have to introduce the planar structure into our single-site model. We have a chain of single-site models as depicted in Fig. 2. The interaction between neighboring planes occurs through the electron-phonon interaction (see Eq. (8)). In the AO model we neglect the interplane hopping and therefore the self-consistent G_0 is plane-diagonal. Eq. (10) can be generalized as

$$\mathcal{G}(\omega) = \left[\frac{1}{G_0^{-1}(\omega) - \xi_\alpha - \hat{\Sigma}^\alpha_{eph}(\omega)} \right]_\xi \quad , \tag{16}$$

where α is the plane index. Notice that after averaging $\mathcal{G}$ does not depend on the plane indexes.

Now we have to generalize Eq. (13) to the BM model. Defining the upper and lower local phonon propagators as

$$D^{(\pm)}(t) = -i \langle T x_{i,\alpha\pm 1/2}(t) x_{i,\alpha\pm 1/2}(0) \rangle \quad , \tag{17}$$

the Fock and Hartree terms of the electron-phonon self-energy take the form

$$\begin{aligned} \hat{\Sigma}^\alpha_F(\omega) = & -\frac{g^2}{2\beta} \sum_m D^+(\omega - \imath\omega_m) \hat{\mathcal{G}}^\alpha(\imath\omega_m) - \\ & -\frac{g^2}{2\beta} \sum_m D^-(\omega - \imath\omega_m) \hat{\mathcal{G}}^\alpha(\imath\omega_m) \quad , \end{aligned} \tag{18}$$

$$\begin{aligned} \hat{\Sigma}^\alpha_H = & \frac{g^2}{2} \left(D^+(0) \hat{n}^\alpha - D^-(0) \hat{n}^{\alpha+1} \right) + \\ & \frac{g^2}{2} \left(D^+(0) \hat{n}^\alpha - D^-(0) \hat{n}^{\alpha-1} \right) \quad , \end{aligned} \tag{19}$$

where $D^{(\pm)}(i\omega_n)$ are the local phonon propagators in the Matsubara frequencies and $\hat{n}^\alpha = -\frac{1}{\beta} \sum_n \hat{\mathcal{G}}^\alpha(\imath\omega_n) e^{i\omega_n 0^+}$ is the local density on a generic site of the plane α. Notice that $\hat{n}^\alpha$ still depend on the disorder realization. Notice also that interplane coupling occurs due to the Hartree term in the self-energy Eq. (18). After Matsubara's frequency summation the Fock contribution to the self-energy is written as

$$\begin{aligned} \hat{\Sigma}^\alpha_F(\omega) = g^2 \int d\epsilon \hat{A}^\alpha(\epsilon) & \left[\frac{b(\omega_0) + f(\epsilon)}{\omega + \omega_0 - \epsilon + \imath\delta} + \right. \\ & \left. + \frac{b(\omega_0) + 1 - f(\epsilon)}{\omega - \omega_0 - \epsilon + \imath\delta} \right] \quad , \end{aligned} \tag{20}$$

with $\hat{A}^\alpha(\epsilon) = (-1/\pi) \Im \hat{\mathcal{G}}^\alpha(\epsilon)$ being the α-th plane spectral function. The scheme of iteration is basically the same as for the Holstein (LOC) model with an important difference: we have to iterate the self-consistency condition for an array of planes. Adopting periodic boundary conditions, we need 64 planes to achieve convergence for the sets of parameters used throughout the paper.

C. Generalization to non-local models of electron-phonon interaction

Now let us consider a general non-local electron-phonon interaction as that of the model NLOC Eq. (3). The perturbation theory in terms of the electron-phonon coupling constant $g_{i,j}$ can be written in the lattice space. This is shown diagramatically in Fig. 1. The diagrams sets are divided into two groups: a) refers to local type diagrams in which only the $[g^2]_{n,n}$ appears (see discussion about the LOC model) while b) contains extra terms which include $[g^2]_{n,m}$ for $m \neq n$. We divide our calculation into two steps.

In a first step we implement the PPNCACPA previously described for the Holstein (LOC) model taking into

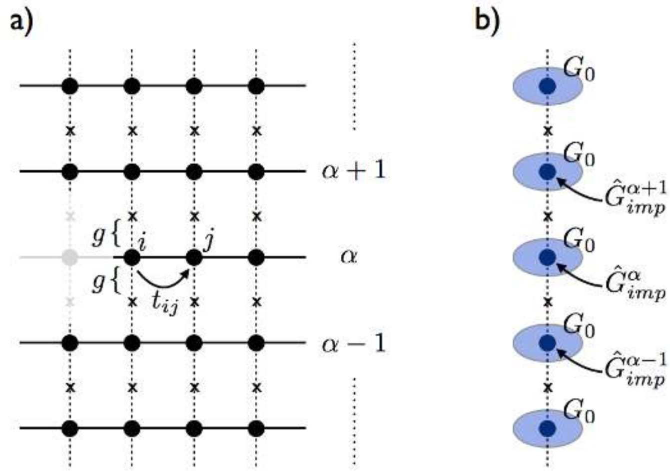

FIG. 2: DMFT mapping of the AO model. a) Lattice model in which electrons move on the planes and interact with the AO phonon. b) Mapping of the lattice problem into a single chain single-site model.

account the a) diagrams for the electron-phonon interaction. We use in this stage a coupling constant $g^2 = [g^2]_{i,i}$. Within such a treatement, we are taking into account disorder and electron-phonon interaction at the local level. Now we include the non-local part of electron-phonon interaction including diagrams of type b) *at the average level*, i.e. we consider the internal propagator averaged over disorder. Average restores translational invariance and the Hartree term (tadpole diagram in Fig. 1b)), which is independent on frequency, can be reabsorbed in the definition of the chemical potential. The only relevant term is the Fock one averaged over disorder, as depicted in Fig. 1b) and highlighted by the blue arrow. The self-energy thus takes into account both disorder and electron-phonon interaction, while disorder and local part of electron-phonon interactions (diagrams a)) are evaluated self-consistently; the non-local part is taken into account non-selfconsistently on a final stage. Therefore this approach should not be extended to the polaronic type of couplings. However, due to the relevance of disorder in our calculations, we have checked that the results are quite insensible to the actual value of the screening wavevector provided that $\kappa > 0.001$, and thus on the specific form of the non-local e-ph coupling.

D. Alternative CPA schemes

In order to investigate the correlations in the one particle spectra between disorder and electron-phonon interaction, in the local PPNCACPA loop we can compare two CPA schemes, the one we are actually using in which the electron-phonon self-energy do depend on local random potentials (CPA2) and a more simpler scheme in which we average the e-ph self-energy diagrams of type a) on disorder (CPA1). In the case of NLOC models, to take into account the non-locality of the electron-phonon interaction, we finally implement the second stage of our approximation having the local self-energy from CPA2 or CPA1 formulations. Notice that CPA1 scheme in absence of electron-phonon interaction is usually referred as *virtual-crystal* approximation[43]. The comparison between the two schemes sill give us an idea of the relevance of the electron-phonon self-energy fluctuations due to disorder at different energy scales.

We notice that, averaging the internal propagators appearing in diagrams of type a) shown in Fig. 1, means substituting the internal electron propagators with their averages. The Hartree contribution (tadpole diagram in fig. 1a)) averages to a frequency and k-independent value thus reducing to a mere shift of the chemical potential. The remaining contribution is the Fock term in which the internal propagator has been averaged over disorder. This average procedure neglects i) correlations between the density and the disorder variable at a given site and ii) disorder and electron-phonon correlated scatterings. From a perturbative point of view the diagrams which contribute to these two mechanisms are depicted in Fig. 3. We notice that, due to our strong-disorder approach,

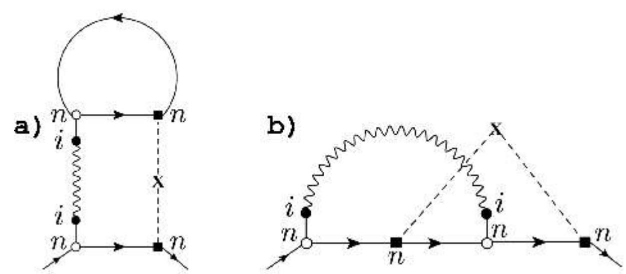

FIG. 3: Examples of diagrams neglected in CPA1 scheme for gaussian distributed disorder. a) A correction which takes into account disorder correlations in the Hartree part of the self-energy entering in Eq. (10) within CPA2 scheme but neglected in the same expansion within CPA1 scheme. Solid line represents the self-consistent propagator G_0, wavy line the phonon propagator, dashed line disorder insertion. b) A disorder-induced vertex correction appearing in the expansion of the Fock part of the local electron-phonon self-energy.

these contributions are not included in the self-consistent Born approximation approach of ref.[27].

IV. RESULTS

Here we present results obtained using basically two kinds of disorder. We first consider a dichotomic disorder (P_i distribution) in which a percentage $x = 5\%$ of sites have a lower energy $E_b = -0.5$ (in unit of the half bandwidth) than all the other sites. This kind of disorder mimics the introduction of impurities associated with doping. To this aim we fix the filling factor to the same value x. We also consider gaussian uncorrelated disorder (P_g distribution) which can mimic a strong structural disorder, as usually happens in thin films. Even if 5% of impurities seems to be a rather small quantity, it can affect severely the lower part of the energy spectrum as can be seen in Fig. 4. Moreover this is precisely the energy range in which electron-phonon interaction is relevant ($\omega \simeq \omega_0$).

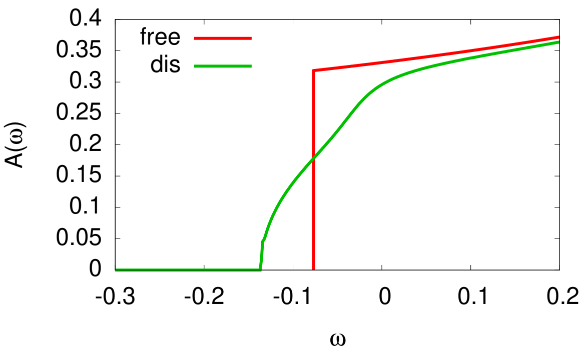

FIG. 4: DOS, $A(\omega)$, of the non-interacting system (free) shifted to match the filling of the 5% doped system (dis). Unit of frequency is D; the zero of frequency is set to the chemical potential.

On top of this disordered system we consider a weak electron-phonon interaction $\lambda = 0.22$, which is the same in all the considered models. To disentangle the separate action of electron-phonon and disorder we show the spectral function in the case of LOC model in Fig. 5. There the spectral function is compared along a cut on k_x axis around the Γ point in the presence of electron-phonon interaction only (panel a)), in the presence of impurities without electron-phonon interaction (panel b)) and under the action of both electron-phonon and impurity-disorder in panel (c)). It's immediately seen that the spectra in panel c) cannot be obtained by a simple broadening of the spectra of panel a). A complete redistribution of the spectral weight is obtained under the action of a quite low electron-phonon coupling in presence of disorder. The growing of an impurity band appears to be evident at the bottom of the coherent electronic band with a merging around the chemical potential. On the other hand, the action of such a strong disorder does not prevent the typical fingerprints of the electron-phonon interaction, as the kinks at the phonon frequency (see Appendix A). This result highlights the fact that when disorder and electron-phonon coupling interact at the same energy scales, as in the considered case, the action of disorder cannot be taken into account as a simple broadening of the spectral features in absence of disorder, since disorder and electron-phonon interaction work in a cooperative way.

In panel d) we plot the spectra obtained using a gaussian disorder with $\sigma^2 = 0.08$. We have chosen the variance of disorder requiring the same value of the Fermi k_F as that given by the 5% impurities. In this case an energy-dependent broadening can be seen in the picture while the phonon signature, even weak, is still visible. Clearly the interplay of impurities and distributed gaussian disorder with electron-phonon interaction is very different.

The scenario presented in Fig. 5 is rather general; indeed it holds also in the case of highly non-local electron-phonon interaction. In Fig. 6 we have considered an electron-phonon interaction of the kind of Eq. (5) with the screening k-vector $\kappa = 10^{-3}$. Comparing the spectra in absence of disorder (Fig. 5 a) and 6 a)) we see that the enhanced forward scattering present in the NLOC model broadens the low-energy features around the Γ point. However in the presence of impurities (Fig. 5 c) and 6 b)) the spectra look much more similar even if phonon signatures are more marked in the NLOC model. This is consistent with the relevance of such a strong disorder at the highest binding energies. Increasing the screening, the range of electron-phonon interaction reduces, and the qualitative scenario becomes increasingly similar to that of LOC model. With the chosen values of parameters at $\kappa = 10^{-2}$ the spectra are almost indistinguishable from those of Fig. 5.

A quantitative measure of the interplay between electron-phonon and disorder effects can be probed by measuring the deviation of the Fermi wave-vector (k_F) from that predicted by Luttinger's theorem[44] at a given electron density. In Fig. 7 (upper panel) the momentum distribution curve (MDC) is obtained from the spectral function. The Luttinger's prediction for k_F coincides with the position of the peaks in the presence of electron-phonon interaction only. Indeed in this case the damping at the Fermi energy is zero and the Fermi surface area is conserved; thus the sole presence of electron-phonon interaction does not lead to a Fermi vector reduction. Disorder alone, even strong as in our case, contributes to a decreasing of k_F only by 10%, while the additional presence of a relatively weak electron-phonon interaction dramatically reduces k_F by 60%. If one takes the Luttinger's theorem[44] for granted in this conditions, the obtained electron density is far from the nominal one given by the impurities' concentration. These evidences should be carefully taken into account for the interpretation of experimental ARPES spectra, being the fingerprint of a strong interplay between disorder and electron-phonon interaction[14]. In the lower panel of Fig. 7 is shown a comparison of the MDC curves for the LOC, NLOC and AO models. We see that the reduction of k_F is less effective in NLOC and AO models compared to LOC one. We will discuss the reason for this behaviour below.

The cooperative action of electron-phonon and disorder interactions is particularly evident in the disorder-induced metal-insulator transition that occurs as a function of the electron-phonon coupling λ. In this work, the disorder-induced MIT is defined looking at the vanishing of the Fermi vector k_F. A vanishing k_F is a precursor of a vanishing density of states at the Fermi level, which in turn leads to an insulating state. It is well known that,

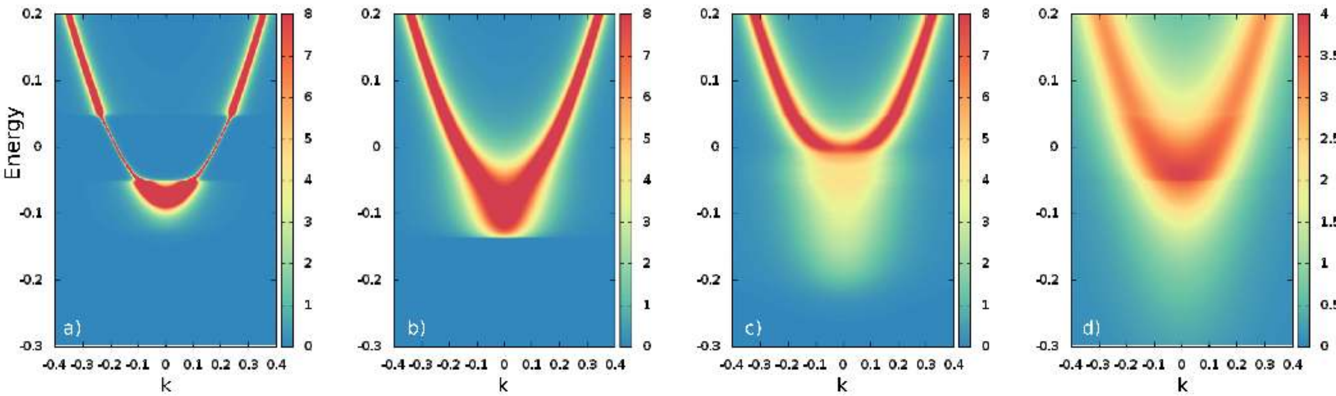

FIG. 5: The spectral function $A(k, \omega)$ for the LOC model. a) Electron-phonon interaction only $\lambda = 0.22$ b) Disorder only c) Electron-phonon interaction + disorder d) Electron-phonon interaction + gaussian disorder, the colourmap (range of z) has been expanded in this case to take into account the lower value of the spectral function.

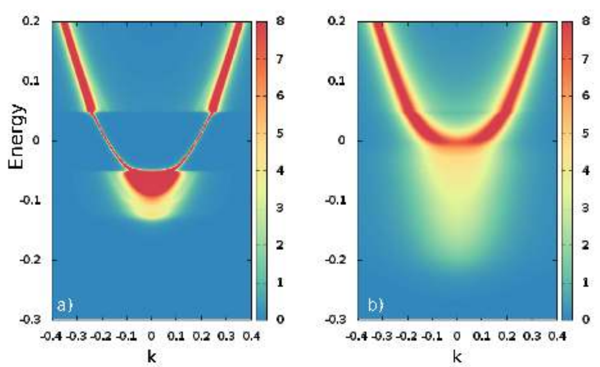

FIG. 6: The spectral function $A(k, \omega)$ for the NLOC model. a) Electron-phonon interaction only $\lambda = 0.22$ b) Electron-phonon interaction + disorder

in a disordered system, increasing the binding energy of the impurities will produce a metal-insulator transition in which an impurity band detaches from the conduction band[45]. Here we achieve the same phenomenon using the synergistic action of electron-phonon interaction as it is shown in Fig. 8 for two different impurity concentrations.

For a given value of $E_b = -0.5$ we report the DOS which clearly opens a gap at $\lambda = 0.275$ in Fig. 9 (upper panel). The vanishing of the Fermi surface occurs at a lower value of λ as it is shown in the inset of the same figure. The synergistic work of electron-phonon interaction originates from the action of the Hartree term Eq. (12) which provides an electron-phonon induced increasing of the binding energy which is proportional to the carrier density at a given site. This is correlated with the presence of the impurity since the density will be higher just at the impurity sites (see Appendix B). When electron-phonon-interaction is non-local this effect is less marked as can be seen in Fig. 9 (lower panel). For instance in the AO model, as the Hartree energy Eq. (18) does depend on the density on nearest neighbor planes along the chain, the interplay between electron-phonon interaction and disorder is less effective, as seen also in the smaller reduction of the Fermi surface with respect to the LOC model (see Fig. 7 lower panel).

Moreover, a further insight into the interplay between electron-phonon and disorder interaction can be obtained by the comparison of our results within the two CPA schemes (see Section III). The DOSs and the spectra obtained by CPA1 and CPA2 approximations are compared in Fig. 10 (upper and lower panels respectively). We see how the interplay between e-ph interaction and disorder affect the DOS below the Fermi energy, just in the energy region in which both disorder and e-ph are present. Noticeably phonon signatures appear much more evident in the CPA2 scheme, and a large spectral weight redistribution occurs at higher binding energies. Moreover we see that within CPA1 scheme the effect of disorder is largely dominant, as can be seen by comparing the spectrum of Fig. 10 (lower left panel) and that obtained in the presence of pure disorder (see Fig. 5 c)). Since in CPA1 we average the electron-phonon self-energy over the disorder variable we can ascribe the large discrepancies between the spectra in Fig. 10 to the correlation between electron-phonon and disorder effects in the self-energy. This issue can be analyzed from the point of view of perturbative expansions. The resummation in CPA2 scheme of diagrams of type a) in Fig. 3 which take into account the correlation at the Hartree level be-

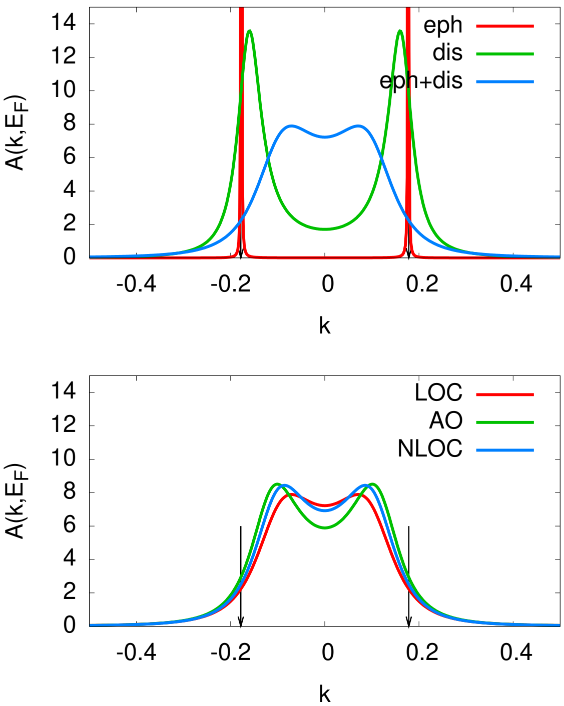

FIG. 7: Upper Panel: an MDC scan at Fermi energy in the LOC model. (eph) stands for the non-disordered system under the action of electron-phonon interaction only. (dis) is the purely disordered system without electron-phonon interaction. (eph+dis) is the system under the action of both electron-phonon and disorder. Lower Panel: an MDC scan at Fermi energy in the LOC compared with NLOC and AO model for the same value of electron-phonon coupling $\lambda = 0.22$ and the same disorder variables $x = 0.05, E_b = -0.5$. Vertical arrows mark the Luttinger's theorem value for k_F.

tween electron-phonon and local disorder, leads to an enhancement of the electron-phonon interaction effects on the energy scale of the emerging impurity band (around $\simeq E_b$ from the Fermi level). In contrast to CPA1 the CPA2 Hartree term is correlated to the presence of the impurity leading to the λ dependence of the disorder-induced metal-insulator transition (see discussion above and upper panel of Fig. 9). For this reason, as shown in Fig. 10, the impurity band within CPA2 seems to be more marked than that in CPA1. However another aspect is clear from the comparison in Fig. 10: the CPA2 impurity band is also much wider that that obtained within CPA1, and, despite the strong disorder, prominent phonon signatures are still evident on the impurity band. This should be ascribed to the correlation between disorder and electron-phonon self-energy at the Fock level diagrams of type b) in Fig. 3. In previous work an interplay between electron-phonon interaction and disorder has been found within self-consistent Born approximation[27–29] in which, despite the self-energy separates into electron-phonon and disorder parts, non ad-

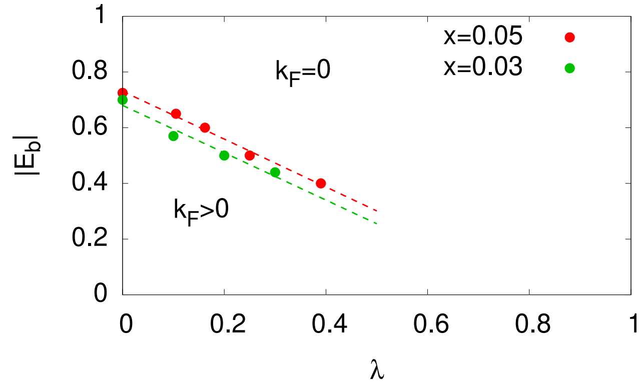

FIG. 8: The phase diagram of the LOC model at zero temperature for $x = 0.03$ ans $x = 0.05$. Points are obtained at values of parameters such that $k_F = 0$. Dashed lines are linear fits of the data. At a given value of λ the increase of impurity concentration stabilizes the conductive phase.

ditivity in electron scattering time is found due to the self-consistency condition. We remark here the difference in our strong-disorder approach in which the self-energy appearing in Eq. (14) is no longer separable into two contributions. We thus have analyzed the strong fluctuations of the self-energy due to disorder rather than its separability into electron-phonon and disorder part.

V. CONCLUSIONS

In conclusion, in this work we have investigated the role of the electron-phonon interaction in disordered systems, and their strong interplay when the energy scales in which they act are comparable. It is well known that trapping impurities provide the necessary energy for the polaronic transition stabilizing the polaronic state at weaker electron-phonon coupling[23–26]. Here we have discussed this interplay at finite electron density and weak electron-phonon coupling, thus relying our study on the PPNCA to deal with weak electron-phonon interaction. We have developed a theoretical method to combine the PPNCA with the CPA to study strongly disordered systems, and we have extended such theory to the Apical Oxygens model[37] and to a non-local electron-phonon interaction characteristic of couplings with crystal's polar modes. We mainly focused our attention on low dimensional systems such as quasi twodimensional or layered ones, since in these cases the effect of disorder can in principle be larger with respect to purely 3D systems. On the other hand, we concentrated on low doped systems in which the impurity band can be very close, and hybridizes, with the bottom of the electronic one. This peculiar, but quite common experimental and theoretical evidence[7–9,14–17] allowed us to study when disorder and electron-phonon interaction act in a cooperative way,

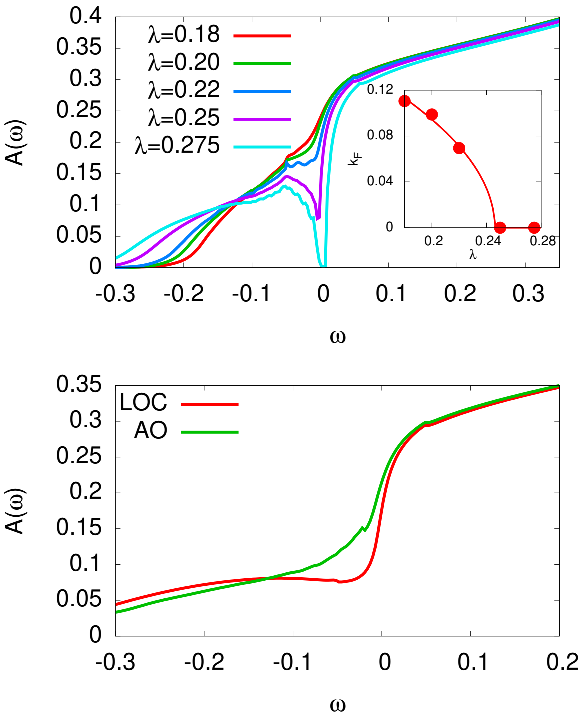

FIG. 9: Upper panel: the interacting density of the states for $x = 0.05$ and disorder level $E_b = -0.5$ as a function of electron-phonon coupling λ. In the inset is shown the value of k_F as a function of λ. Lower panel: The DOS of the LOC and AO models at $\lambda = 0.3$, here a gaussian disorder of std. deviation $\sigma = 0.05$ has been added to the dichotomic disorder.

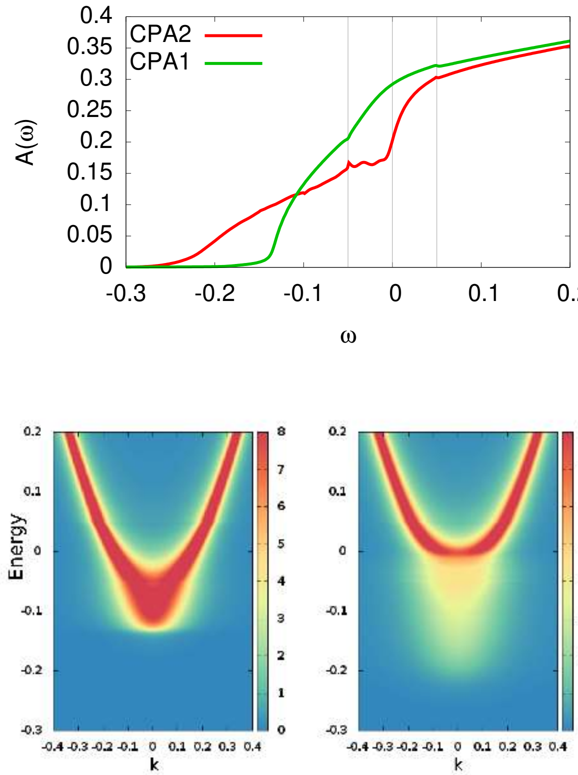

FIG. 10: Upper panel: DOS of LOC model within CPA1 and CPA2 approximations,vertical dotted lines marks the Fermi energy ($\omega = 0$) and the two phonon resonances at $\pm\omega_0$. Lower panel: Comparison of CPA1 (left) and CPA2 (right) spectra.

and the action of disorder cannot be included in a perturbative way as a source of weak broadening of the spectral features. On the contrary, impurity-type disorder strongly affects the electronic structure giving rise to a significant spectral weight redistribution. This could lead to a dramatic Fermi surface reduction even at moderate electron-phonon couplings, which in turns can be detected as a Luttinger's theorem violation[14] and eventually an electron-phonon driven metal-insulator transition as the Fermi surface vanishes. From a quantitative point of view, the strongest interplay between electron-phonon and local disorder is found for the local electron-phonon interaction (LOC model). Non-local couplings studied in this work (AO, NLOC) both display a less effective interplay with disorder as a consequence of the interactions' non-locality.

CPA approximation used to approach the strong disorder regime is a reasonable approximation for the DOS or the average spectral function in three dimensions[46]. In our 2 (LOC,NLOC) or 2+1 (AO) dimensional systems there are however some deviations which can be treated within a non-local DCA framework[47]. Generally speaking CPA overestimates the disorder induced gap. As a consequence in our treatment of the disorder-induced MIT we expect that the disorder needed to reach the MIT would be slightly lower going beyond CPA. Localization effects, absent in CPA approach, which are however beyond the present work, can be relevant for transport properties in low dimensional systems. Their effects can be probed at the local level by anomalous fluctuations of the local DOSs which can be relevant to tunneling experiments. Instead of the averaged DOS taken into account in this work one can consider the typical DOS obtained as geometric averages of local DOSs[46]. As far as local quantities are concerned for the LOC model one can generalize our self-consistency equations to the case of typical quantities following the lines of refs.[46,48].

PPNCA approximation for electron-phonon interaction used in our work cannot be used to attach the polaronic regime which can be interesting to study, since the recently found polaronic resonances in single layer high-T_c superconducting $FeSe$[10]. Also from a theoretical point of view, the interplay between disorder and polaronic electron-phonon interaction could be much different from that proposed in the present paper[37]. To this aim a beyond-NCA approach such as DMFT should be useful also to include electronic correlations. A cluster-DMFT approach could also be useful to include spatial correlations which we neglect in our local approach in the

LOC model case, overcoming in this way the well known problems of single site DMFT in dealing with systems at low dimensionality[49].

The authors kindly thank Prof. K. Shen and Dr. Y. Nie for very helpful discussions and hints on the work. Helpful discussions with Dr. E. Cappelluti, Dr. P. Barone, Prof. G. Sangiovanni and Prof. R. Valentí are also acknowledged. The computational support from the CINECA supercomputing center under the grant "ConvR_aq_caspF" is gratefully acknowledged.

---

* Electronic address: domenico.disante@aquila.infn.it
† Electronic address: sergio.ciuchi@aquila.infn.it

1 A. Damascelli, Z, Hussain and Z. X. Shen, Rev. Mod. Phys. **75**, 473 (2003)
2 T. Cuk, D. H. Lu, X. J. Zhou, Z.-X. Shen, T. P. Devereaux, and N. Nagaosa, phys. stat. sol. (b) **242**, 11 (2005)
3 E. Dagotto, T. Hotta and A. Moreo, Physics Report **334**, 1 (2001)
4 Y. Tokura, Physics Today, July 2003, pp 50-55.
5 M. Z. Hasan and C. L. Kane, Rev. Mod. Phys. **82**, 3045 (2010)
6 A. H. Castro Neto, F. Guinea, N. M. R. Peres, K. S. Novoselov and A. K. Geim, Rev. Mod. Phys. **81**, 109 (2009)
7 Young Jun Chang, Aaron Bostwick, Yong Su Kim, Karsten Horn, and Eli Rotenberg Phys. Rev. B **81**, 235109(2010)
8 W Meevasana, X J Zhou, B Moritz, C-C Chen, R H He, S-I Fujimori, D H Lu, S-K Mo, R G Moore, F Baumberger, T P Devereaux, D van der Marel, N Nagaosa, J Zaanen and Z-X Shen, New J. of Phys. **12**, 023004 (2010)
9 M. Takizawa, K. Maekawa, H. Wadati, T. Yoshida, and A. Fujimori H. Kumigashira and M. Oshima, Phys. Rev. B **79**, 113103 (2009)
10 J. J. Lee, F. T. Schmitt, R. G. Moore, S. Johnston, Y.-T. Cui, W. Li, M. Yi, Z. K. Liu, M. Hashimoto, Y. Zhang, D. H. Lu, T. P. Devereaux, D. -H. Lee, Z.-X. Shen arXiv:1312.2633
11 S. Moser, L. Moreschini, J. Jaćimović, O. S. Barišić, H. Berger, A. Magrez, Y. J. Chang, K. S. Kim, A. Bostwick, E. Rotenberg, L. Forró, and M. Grioni Phys. Rev. Lett. **110**, 196403 (2013)
12 R. Nourafkan, F. Marsiglio and G. Kotliar, Phys. Rev. Lett. **109**, 017001 (2012)
13 T. Kondo, Y. Nakashima, Y. Ota, Y. Ishida, W. Malaeb, K. Okazaki, S. Shin, M. Kriener, S. Sasaki, K. Segawa and Y. Ando, Phys. Rev. Lett. **110**, 217601 (2013)
14 Y.F. Nie, D. Di Sante, S. Chatterjee, P.D.C. King, M. Uchida, S. Ciuchi, D.G. Schlom, and K.M. Shen in preparation
15 P. Richard, T. Sato, S. Souma, K. Nakayama, H. W. Liu, K. Iwaya, T. Hitosugi, H. Aida, H. Ding, and T. Takahashi, App. Phys. Lett. **101**, 232105 (2012)
16 J. Okabayashi, A. Kimura, O. Rader, T. Mizokawa, A. Fujimori, T. Hayashi, and M. Tanaka, Phys. Rev. B, **64**, 125304 (2001)
17 M. A. Majidi, J. Moreno, M. Jarrell, R. S. Fishman, and K. Aryanpour, Phys. Rev. B, **74**, 115205 (2006)
18 G. Berner, M. Sing, H. Fujiwara, A. Yasui, Y. Saitoh, A. Yamasaki, Y. Nishitani, A. Sekiyama, N. Pavlenko, T. Kopp, C. Richter, J. Mannhart, S. Suga, and R. Claessen, Phys. Rev. Lett **110**, 247601 (2013)
19 A. F. Santander-Syro, O. Copie, T. Kondo, F. Fortuna, S. Pailhés, R. Weht, X. G. Qiu, F. Bertran, A. Nicolaou, A. Taleb-Ibrahimi, P. Le Févre, G. Herranz, M. Bibes, N. Reyren, Y. Apertet, P. Lecoeur, A. Barthélémy and M. J. Rozenberg, Nature **469**, 189 (2011)
20 J. Shen, H. Lee, R. Valentí and H. O. Jeschke, Phys. Rev. B **86**, 195119 (2012)
21 N. Reyren, S. Thiel, A. D. Caviglia, L. Fitting Kourkoutis, G. Hammerl, C. Richter, C. W. Schneider, T. Kopp, A.-S. Rüetschi, D. Jaccard, M. Gabay, D. A. Muller, J.-M. Triscone, and J. Mannhart, Science **317**, 1196 (2007)
22 A. N. Das and S. Sil, Physics Letters A **348**, 266 (2006)
23 J. P. Hague, P. E. Kornilovitch, and A. S. Alexandrov, Phys. Rev. B **78**, 092302 (2008)
24 M. Berciu, A. S. Mishchenko and N. Nagaosa, Eur. Phys. Lett. **89**, 37007 (2010)
25 C. A. Perroni and V. Cataudella, Phys. Rev. B **85**, 155205 (2012)
26 Hadi Ebrahimnejad and Mona Berciu, Phys. Rev. B **85**, 165117 (2012)
27 E. Cappelluti and L. Pietronero, Phys. Rev. B **68**, 224511 (2003)
28 A. Knigavko, J. P. Carbotte, Phys. Rev. B **73**, 125114 (2006)
29 F. Dogan and F. Marsiglio, J. Sup. Nov. Magn. **20**, 225 (2007)
30 A. Chen, G. Weisz, A. Scher, Phys. Rev. B **5**, 2897 (1972)
31 S.M. Girvin, M. Jonson, Phys. Rev. B **22**, (1980)
32 B. M. Letfulov, J. K. Freericks, Phys. Rev. B **66**, 033102 (2002)
33 J. K. Freericks and V. Zlatić Rev. Mod. Phys. **75**, 1333 (2003)
34 It is worth to note that even a modest amount of impurities can introduce strong disorder effects at the energy scale of the order of the impurities' binding energy.
35 S. Das Sarma and B. A. Mason, Annals of Physics **163**, 78 (1985)
36 O. Gunnarsson and O. Rösch, J. Phys.: Condens. Matter **20**, 043201 (2008)
37 Bayo Lau, Mona Berciu, and George A. Sawatzky Phys. Rev. B **76**, 174305 (2007)
38 L. Schwartz and E. Siggia, Phys. Rev. B **5**, 383 (1972)
39 D. Vollhardt, in Correlated Electron Systems, edited by V. J. Emery (World Scientific, Singapore, 1992).
40 A. Georges, G. Kotliar, W. Krauth, and M.J. Rozenberg, Rev. Mod. Phys. **68**, 13 (1996)
41 F. X. Bronold, A. Saxena and A. R. Bishop, Phys. Rev. B **63**, 235109 (2001)
42 To avoid confusion with the acronym NCA used in the theory of strongly correlated electrons system, we name our approximation PPNCA to indicate a theory which includes all non-crossing diagrams with respect to phonon propagator. Notice that our theory includes diagrams in which disorder insertions cross with phonon propagators (see Fig. 3)
43 D. Stroud and H. Ehrenreich, Phys. Rev. B **2**, 3197 (1970)
44 In two dimensions, for a circular Fermi surface, the expression for k_F is $k_F = \sqrt{2x/\pi}$ (in units of (π/a)).

[45] With our choose of DOS at $x = 0.05$ CPA gives $E_b = -0.725$ for the disorder-induced Mott transition.
[46] V. Dobrosavljević, A. A. Pastor and B. K. Nikolić, Europhys. Lett. **62**, 76 (2003)
[47] M. Jarrell and H. R. Krishnamurthy, Phys. Rev. B **63**, 125102 (2001)
[48] H. Fehske, F.-X. Bronold, and A. Alvermann, Proc. Int. School of Physics "Enrico Fermi", Course CLXI, Polarons in Bulk Materials and Systems with Reduced Dimensionality, Eds. G. Iadonisi, J. Ranninger, G. de Filippis, IOS Press, Amsterdam, Oxford, Tokio, Washington DC, 313 (2006); F.-X. Bronold, A. Alvermann and H. Fehske, Phil. Mag. **84**, 673 (2004)
[49] T. Maier, M. Jarrell, T. Pruschke and M. Hettler, Rev. Mod. Phys. **77**, 1027 (2005)

Appendix A: Second derivative of the spectral function

A common used technique to highlight subtle spectral features is to take the second derivative of the spectral function $\frac{\partial^2}{\partial \omega^2} A(\mathbf{k}, \omega)$. In Fig. 11 we plot this function using CPA1 and CPA2 iteration schemes. In both cases the phonon's signatures are evident but a little bit more within CPA2. More importantly at higher binding energies, CPA1 spectra clearly shows disorder non-dispersed features while in CPA2 clear phonon's higher order resonances are visible up to fourth order, even in the presence of such a strong disorder.

Appendix B: Electron-phonon induced Mott transition

Let us consider the bimodal disorder case $P_i(\xi) = x\delta(\xi - E_b) + (1-x)\delta(\xi)$ in the LOC model. Let us consider only the action of the Hartree term in the self-energy Eq. (12), so that the single-site Green function Eq. (10) reads

$$\mathcal{G}(\omega) = \frac{x}{G_0^{-1}(\omega) - E_b + \lambda n_1} + \frac{1-x}{G_0^{-1}(\omega) + \lambda n_0}, \quad \text{(B1)}$$

where

$$n_1 = -\frac{1}{\beta} \sum_n \frac{x}{G_0^{-1}(\omega) - E_b + \lambda n_1} e^{i\omega_n 0^+} \quad \text{(B2)}$$

$$n_0 = -\frac{1}{\beta} \sum_n \frac{1-x}{G_0^{-1}(\omega) + \lambda n_0} e^{i\omega_n 0^+} \quad , \quad \text{(B3)}$$

where n_1 is the electron density in the impurity site and n_0 is the density everywhere else. In the atomic (zero hopping) limit we have $n_1 = 1, n_0 = 0$ but due to the hibridization of the impurity sites $n_1 < 1$ and $n_0 > 0$. From Eqs. (B1,B2,B3) it is evident that as far as the electron-phonon interaction is considered at the Hartree level $E_b \to E_b - \lambda(n_1 - n_0)$ and the disorder-induced metal-insulator transition occurs when

$$|E_b| = |E_{MIT}| - \lambda(n_1 - n_0) \quad \text{(B4)}$$

with $|E_{MIT}|$ the binding energy at the impurity site needed to detach the impurity band in absence of electron-phonon interaction. Eq. (B4) explains the linear dependence found for small λ for the disorder-induced metal-insulator transition in Fig. 8. It is worth to note that this effect is absent in CPA1 where the electron-phonon self-energy is mediated and as a consequence there is no electron-phonon contribution to the binding energy at the impurity site.

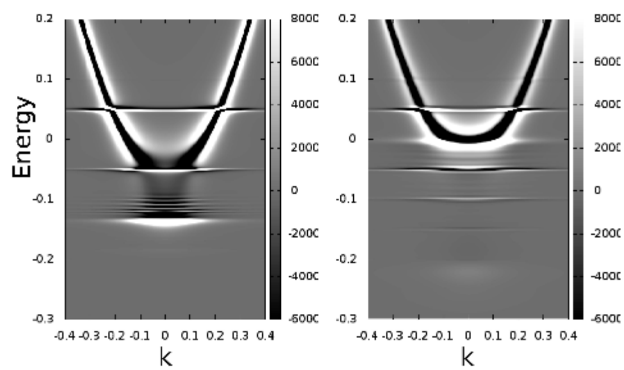

FIG. 11: Comparison of second derivative of the spectral function within CPA1 (left) and CPA2 (right) spectra.